for most forms of the amplitude, although, as found empirically,[2,4,5,12] dependent upon the particular particle which is being scattered.

If the scattering amplitudes consist of the combination of diffractive and resonant parts given by Eqs. (4) and (5) and if the deuteron is again described by a Gaussian wave function, $\langle r^{-2}\rangle_g$ takes a more complicated and weakly energy-dependent form:

$$\langle r^{-2}\rangle_g=\left[\sigma_{\mathrm{diff}}{}^p\sigma_{\mathrm{diff}}{}^n\left(\frac{2}{\gamma+2(\beta^p+\beta^n)}\right)+\sigma_{\mathrm{res}}{}^p\sigma_{\mathrm{res}}{}^n\left(\frac{2}{\gamma}\right)+\sigma_{\mathrm{diff}}{}^p\sigma_{\mathrm{res}}{}^n\left(\frac{2}{\gamma+2\beta^p}\right)+\sigma_{\mathrm{res}}{}^p\sigma_{\mathrm{diff}}{}^n\left(\frac{2}{\gamma+2\beta^p}\right)\right]\Big/\sigma_p{}^{\mathrm{tot}}\sigma_n{}^{\mathrm{tot}}. \quad \text{(B3)}$$

Equation (B3) exhibits a quite natural weighting of the different possible limits of $\langle r^{-2}\rangle_g$.

PHYSICAL REVIEW D VOLUME 3, NUMBER 1 1 JANUARY 1971

Double-Peripheral-Model Analysis of the Reaction* $K^+p\to K^+\pi^-\Delta^{++}{}_{1236}$ at 9 GeV/c

CHUMIN FU†
Lawrence Radiation Laboratory, University of California, Berkeley, California 94720
(Received 26 June 1970)

Using a double-Regge-pole-exchange model, we study the low-$\Delta^{++}\pi^-$-mass enhancement in the reaction $K^+p\to K^+\pi^-\Delta^{++}{}_{1236}$ at 9 GeV/c. We find that P and π double exchange dominate the process. In general the model agrees with the data in the region where $M(K^+\pi^-)\gtrsim 1.54$ GeV, $-t_{KK}<0.5$ (GeV/c)^2, and $-t_{p\Delta}<0.5$ (GeV/c)^2. The possibility of extending the model into the large-t region and problems involved in the extrapolation of the model to the $K\pi$ threshold are investigated. The importance of the contribution from the double-peripheral process in the low-$M(K^+\pi^-)$ region and its implications for the analysis of the $K\pi$ system are discussed.

I. INTRODUCTION

THE general features of the reaction $K^+p\to K^+\pi^-\Delta^{++}{}_{1236}$ at 9 GeV/c were discussed in an earlier paper.[1] In this paper we study the reaction in the high-$K\pi$-mass region $[M(K^+\pi^-)\gtrsim 1.54$ GeV$]$ on the basis of a double-Regge-pole-exchange model. The advantage of this model is that it has the same simple form as a single-Regge-pole-exchange model and theoretically the Regge parameters (except the coupling at the internal vertex) used here can be wholly taken from those that were determined by the data from two-body or quasi-two-body final states. It is well known that a double-Regge-pole model can usually describe the data from three-body or quasi-three-body final states at high energies fairly well. However, in applying the model there are still some unsolved problems.

(a) The commonly used Regge parameters are known only in their order of magnitude. The exact values are not well determined. Hence when one finds that the fits of the model to the data are insensitive to the variation of the parameters, one cannot distinguish whether this is due to the effect of a collective change of the many Regge parameters or due to an incomplete study of the data. Poor statistics of the data and unclean samples can also contribute to the sources of uncertainty.

(b) There is no evidence for Toller-angle dependence at the internal vertex. By the same argument given in (a), it is not clear at all whether there should be a Toller-angle dependence for the Reggeon-Reggeon-particle coupling.

(c) Over how large a range in momentum transfer variables (t's) a peripheral model can extend is not well known.

(d) Granted that duality is a valid concept,[2] how would one extrapolate the model to small subinvariant energies s? Would the extrapolation also be insensitive to a variation of Regge parameters? Answers to these questions are not known either.

In an attempt to understand these problems, we analyze our data in an exhaustive manner. The method and the results of the analysis are presented in Secs. II and III. Section IV discusses the extrapolation of the model to small subinvariant energies. Section V gives our conclusions.

This experiment was carried out in the Brookhaven National Laboratory 80-in. hydrogen bubble chamber,

* Work supported by the U. S. Atomic Energy Commission.
† Present address: Department of Physics, Illinois Institute of Technology, Chicago, Ill. 60616.
[1] C. Fu, A. Firestone, G. Goldhaber, and G. H. Trilling, Nucl. Phys. B18, 93 (1970).
[2] (a) R. Dolen, D. Horn, and C. Schmid, Phys. Rev. 166, 1768 (1968); (b) G. F. Chew and A. Pignotti, Phys. Rev. Letters 20, 1078 (1968).

which was exposed to a 9-GeV/c rf-separated K^+ beam at the AGS. The details of the experiments, the measurements, and the kinematical fitting procedures are described in Ref. 1 and the Ref. 5 therein.

II. MODEL AND METHOD OF ANALYSIS

A. Model

There are many multiperipheral models and phenomenological analyses of the data discussed in the literature.[3,4] Here we adopt the one given in Ref. 3(e). Consider Fig. 1(a), a diagram for the reaction $a+b\to 1+2+3$. The invariant amplitude is

$$A(s,s_1,s_2,t_1,t_2)\approx\beta_1(t_1)\xi_1(t_1)\left(\frac{\tilde{s}_1}{s_{10}}\right)^{\alpha_1(t_1)}\times\beta_2(t_2)\xi_2(t_2)\left(\frac{\tilde{s}_2}{s_{20}}\right)^{\alpha_2(t_2)}\beta_3(t_1,t_2,\omega)\,, \quad (1)$$

where s, s_1, s_2, t_1, and t_2 are as indicated in Fig. 1(a),

$$\tilde{s}_1=s_1-t_2-m_a{}^2+\tfrac{1}{2}t_1{}^{-1}(m_1{}^2-m_a{}^2-t_1)(m_3{}^2-t_1-t_2)\,,$$

and $\tilde{s}_2$ is obtained by interchanging the subscripts 1 and 2. The Toller angle ω is defined by

$$\cos\omega=\frac{\mathbf{p}_a\times\mathbf{p}_1\cdot\mathbf{p}_b\times\mathbf{p}_2}{|\mathbf{p}_a\times\mathbf{p}_1||\mathbf{p}_b\times\mathbf{p}_2|}$$

in the rest frame of particle 3. The α_i's are the Regge trajectories exchanged and

$$\xi_i=\frac{1\pm e^{-i\pi\alpha_i(t_i)}}{\sin\pi\alpha_i(t_i)}\,.$$

The β_i's are the residue functions. The s_{i0}'s are the energy scale constants.

For the reaction $K^+p\to K^+\pi^-\Delta^{++}{}_{1236}$, the allowable exchange pairs (α_1,α_2) are (P,π), (P,A_1), (ρ,π), (ρ,A_2), (ρ,A_1), and (ω,ρ). Consider the (P,π) pair only and assume further that P is a fixed pole with an intercept 1 in the Chew-Frautschi plot. After squaring Eq. (1) and some simplifications, one obtains an intensity

$$I=N_0e^{\gamma t_1}\frac{(\pi\alpha_\pi{}')^2}{1-\cos\pi\alpha_\pi(t_2)}(\tilde{s}_1)^2\left(\frac{\tilde{s}_2}{s_0}\right)^{2\alpha_\pi(t_2)}f(\omega,t_1,t_2)\,, \quad (2)$$

where $\alpha_\pi=\alpha_\pi{}'(t_2-m_\pi{}^2)$ and N_0 is a normalization constant. This equation is the same as that given in Ref. 3(e) provided that we set $f(\omega,t_1,t_2)$ equal to a constant. Here we have replaced s_{10} by unity and s_{20} by s_0. The effect of s_{10} is taken care of by the normalization constant N_0. Other details of the derivation were discussed in Ref. 3(e).

Since the Pomeranchukon is not well understood at present and five exchange pairs other than (P,π) are also allowed, for $K^+\pi^-$ mass between 1.54 and 2.8 GeV it is reasonable to replace $(\tilde{s}_1)^2$ by $(s_1)^{2c}$ in Eq. (2), where c is a constant parameter.

Using the notations indicated in Fig. 1(b), we rewrite Eq. (2) as

$$I=N_0e^{\gamma t_{KK}}\frac{(\pi\alpha'_\pi)^2}{1-\cos\pi\alpha_\pi(t_{p\Delta})}(\tilde{s}_{K\pi})^{2c}\left(\frac{\tilde{s}_{\Delta\pi}}{s_0}\right)^{2\alpha_\pi(t_{p\Delta})}\times f(\omega,t_{p\Delta},t_{KK})\,, \quad (3a)$$

which is to be used in this analysis. We assume that f takes the form

$$f=[1+a(t_{p\Delta}/m_\pi{}^2)\cos\omega]^2\,, \quad (3b)$$

where a is a constant parameter. Equation (3b) is purely empirical. It has the property that f has no Toller-angle dependence at $t_{p\Delta}=0$, which is required on a theoretical basis.[5] In this analysis, there are five parameters involved, i.e., γ, $\alpha_\pi{}'$, c, s_0, and a. Two cases are considered, namely,

Case I: $a=0$,

Case II: a is a free parameter.

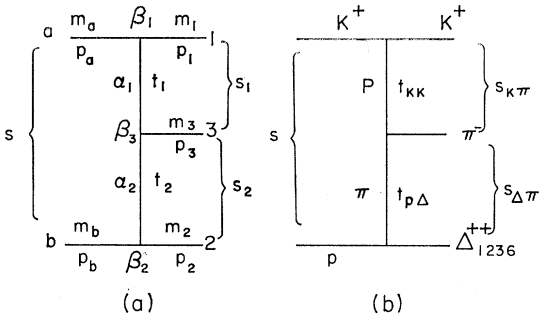

FIG. 1. Double-Regge-pole-exchange diagram for (a) a reaction $a+b\to 1+2+3$ and (b) the reactions $K^+p\to K^+\pi^-\Delta^{++}{}_{1236}$.

[3] (a) N. F. Bali, G. F. Chew, and A. Pignotti, Phys. Rev. Letters **19**, 614 (1967); Phys. Rev. **163**, 1572 (1967); (b) Chan Hong-Mo, K. Kajantie, and G. Ranft, Nuovo Cimento **49**, 157 (1967); E. Flamino, *ibid.* **51**, 696 (1967); (c) Review talks given by Chan Hong-Mo and S. Ratti, in *Proceedings of the Topical Conference on High-Energy Collisions of Hadrons, CERN, 1968* (Scientific Information Service, Geneva, 1968); (d) Review talks by Chan Hong-Mo and O. Czyzewski, in *Proceedings of the Fourteenth International Conference on High-Energy Physics, Vienna, 1968*, edited by J. Prentki and J. Steinberger (CERN, Geneva, 1968); (e) Review talk given by J. D. Jackson, in *Proceedings of the Lund International Conference on Elementary Particles, Lund, Sweden, 1969*, edited by G. von Dardel (Berlingska Boktryckeriet, Lund, Sweden, 1969); (f) G. Ranft, Fortschr. Physik **18**, 1 (1970); (g) E. L. Berger, Phys. Rev. **178**, 1567 (1969).

[4] For double-peripheral-model analyses on $K\pi\Delta^{++}$ final states, see (a) G. Bassompierre *et al.*, Nucl. Phys. **B14**, 143 (1969) on the reaction $K^+p\to K^+\pi^-\Delta^{++}$ at 5 GeV/c; (b) J. Andrews, J. Lach, T. Ludlam, J. Sandweiss, H. D. Taft, and E. L. Berger, Phys. Rev. Letters **22**, 731 (1969) on the reaction $K^-p\to K^-\pi^-\Delta^{++}$ at 12.6 GeV/c. Many phenomenological analyses on the other reactions were reviewed in Refs. 3(b)–3(e).

[5] J. M. Kosterlitz, Nucl. Phys. **B9**, 273 (1969).

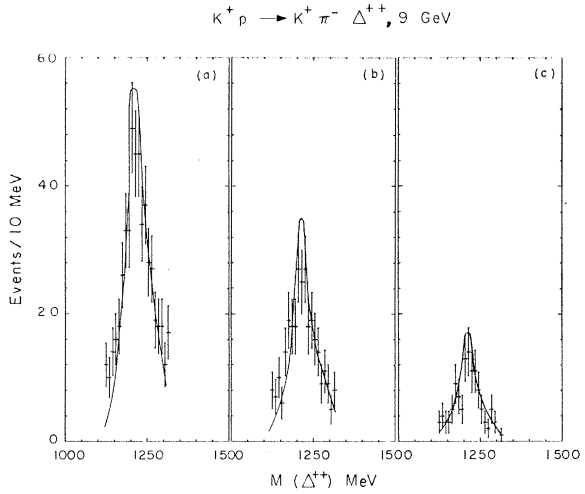

FIG. 2. Mass distributions for $\Delta^{++}{}_{1236}$ (1120 to 1320 MeV) for samples (a) A, (b) B, and (c) C. The solid curves show the distributions for Monte Carlo events.

B. Method of Analysis

In comparing the data with the theoretical calculations, we follow the procedures below.

(1) Generate Monte Carlo events for the $K^+\pi^-\Delta^{++}{}_{1236}$ final states with a variable mass for the $\Delta^{++}{}_{1236}$ given by a Breit-Wigner distribution.[6]

(2) Assign to each Monte Carlo event a weight according to Eq. (3a).

(3) Compare the various distributions from the Monte Carlo events with those from the data, and vary the parameters in Eq. (3a) until we obtain the best fit for all those distributions considered. The goodness of the fit is determined by a χ^2 calculation.[7]

In order to investigate the problems stated in the Introduction, we choose to study the following three samples with $M(K^+\pi^-)>1.54$ GeV:

Sample A: $-t_{K^+K^+}$ and $-t_{p\Delta^{++}}<1.0$ $(\mathrm{GeV}/c)^2$ (511 events),

Sample B: $-t_{K^+K^+}$ and $-t_{p\Delta^{++}}<0.5$ $(\mathrm{GeV}/c)^2$ (287 events),

Sample C: $-t_{K^+K^+}$ and $-t_{p\Delta^{++}}<0.3$ $(\mathrm{GeV}/c)^2$ (115 events).

[6] A Breit-Wigner distribution of the form $M_0\Gamma/[(M_0^2-M)^2+\Gamma^2M_0]$ with $\Gamma=(\Gamma_0/M)(p/p_0)^3(am_\pi^2+p_0^2)/(am_\pi^2=p^2)$ is used. The M is the $p\pi^+$ invariant mass. The M_0 is the mass of M at resonance. The p and p_0 are the momenta of the proton in the $p\pi^+$ c.m. system at masses M and M_0, respectively. Here we take $M_0=1236$ MeV, $\Gamma_0=120$ MeV, and $a=1$. Detailed discussions on the phenomenological analysis of resonances are in J. D. Jackson, Nuovo Cimento **36**, 1644 (1964).

[7] $\chi^2=\sum_{i=1}^{N}[(N_D{}^i-N_{MC}{}^i)N_{MC}]$, where the $N_D{}^i$ and the $N_{MC}{}^i$ are the number of events from the data and the Monte Carlo calculation of the model in the ith bin of a distribution. Owing to the statistical fluctuations, we combine several bins into one in some cases.

The N_0 is determined by normalizing to sample B the Monte Carlo events with the same kinematic cuts as those imposed on sample B. The parameters γ, α_π', c, s_0, and a are obtained by comparing the distributions of 12 variables from the events in sample B with those from the corresponding Monte Carlo events [three invariant masses, $M(K^+\pi^-)$, $M(\Delta^{++}\pi^-)$, and $M(K^+\Delta^{++})$, four four-momentum transfers, $-t_{KK}$, $-t_{p\Delta}$, $-t_{K\pi}$, and $-t_{p\pi}$, and five angular variables, $\cos\theta(K^+\pi^-)$, $\phi(K^+\pi^-)$, $\cos\theta(\Delta^{++}\pi^-)$, $\phi(\Delta^{++}\pi^-)$, and ω]. θ and ϕ are, respectively, the Jackson angle and the Treiman-Yang angle for a two-particle composite. If the model is valid and the parameters obtained are correct, then one should

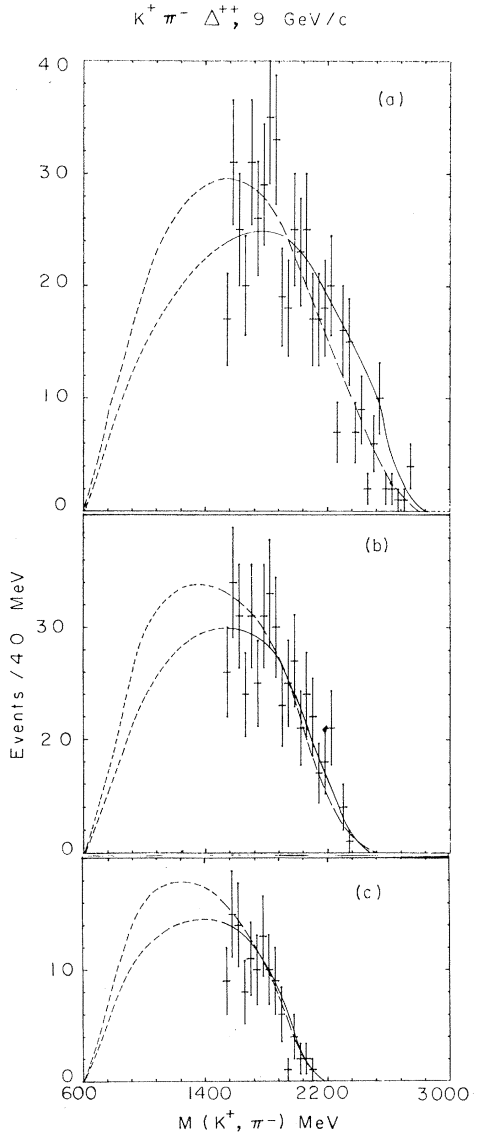

FIG. 3. $K^+\pi^-$ mass distributions for samples (a) A, (b) B, and (c) C. The solid and the long-dash curves correspond to cases I and II, respectively. The short-dash curves are the extrapolation of cases I and II.

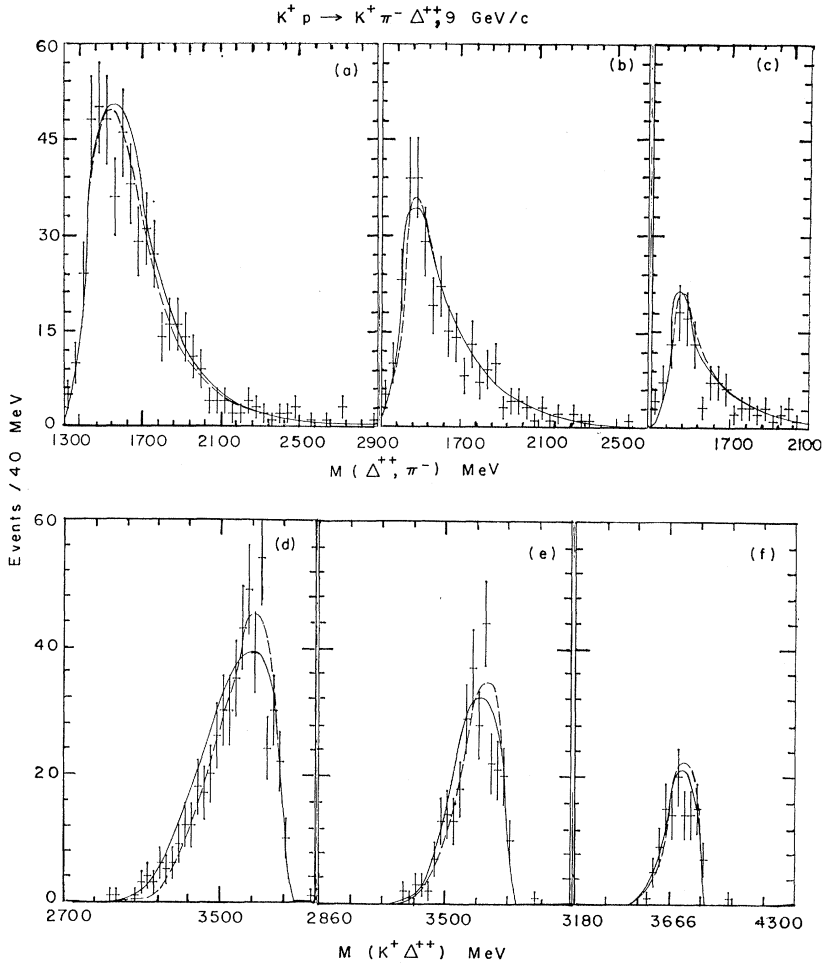

FIG. 4. $\Delta^{++}\pi^-$ mass distributions for samples (a) A, (b) B, and (c) C and $K^+\Delta^{++}$ mass distributions for samples (d) A, (e) B, and (f) C. The solid and the long-dash curves, the results from the model, have the same meaning as those shown in Fig. 3.

expect good agreements between the various distributions from the Monte Carlo events and those from the data in any t region where the t values are smaller than those of sample B. Furthermore, one can also test the validity of the model in a large-t region by extending the t cuts imposed on the data and the Monte Carlo events. These are the motivations for studying samples C and A. In principle one should compare the model with the data in different noninclusive t intervals. Because of the statistical limitations of our data, we choose only the t criteria described earlier.

III. RESULTS

Various values for the parameters in Eq. (3a) have been tried; the best values obtained are Case I: $a=0$, $\gamma=4$ (GeV/c)$^{-2}$, $\alpha_\pi'=1.2$ (GeV/c)$^{-2}$, $s_0=1.0$ GeV^2, and $c=0.85$; Case II: $a=0.015$, $\gamma=3.2$ (GeV/c)$^{-2}$, $\alpha_\pi'=1.12$ (GeV/c)$^{-2}$, $s_0=1.0$ GeV^2, and $c=0.85$.

A. Distributions of Various Kinematic Variables

For each variable the distributions are to be presented in the order of samples A, B, and C. The corresponding distributions from the Monte Carlo events are shown in solid lines for case I and long-dash lines for case II.

Figure 2 shows the $\Delta^{++}{}_{1236}$ mass distributions. Here we check whether the Monte Carlo events generated for the $K^+\pi^-\Delta^{++}{}_{1236}$ final state indeed have a $p\pi^+$ mass distribution similar to that of the samples. Comparing the data with the curve shown in Fig. 2(b), we obtain a $\chi^2=16.4$ and a confidence level$=12.6\%$ with 14 degrees of freedom. (We consider M_0, Γ_0, and a as parameters in the Breit-Wigner distribution discussed in Ref. 6. The curves corresponding to case I and case II are very close; therefore, only the result of case I is shown in Fig. 2.)

Figures 3(a), 3(b), and 3(c) show the $K^+\pi^-$ mass spectra for samples A, B, and C, respectively. The short-dash lines are the extrapolations of the model calculations to the region where $M(K^+\pi^-)<1540$ MeV. Discussions of the extrapolation are given in Sec. IV. In Fig. 3(b) the two curves are close in the region where $M(K^+\pi^-)\gtrsim 1700$ MeV. Below 1700 MeV in the $K^+\pi^-$ mass, the two curves start to deviate. The deviation between the solid and the long-dash lines becomes larger for sample A and smaller for sample B. This seems

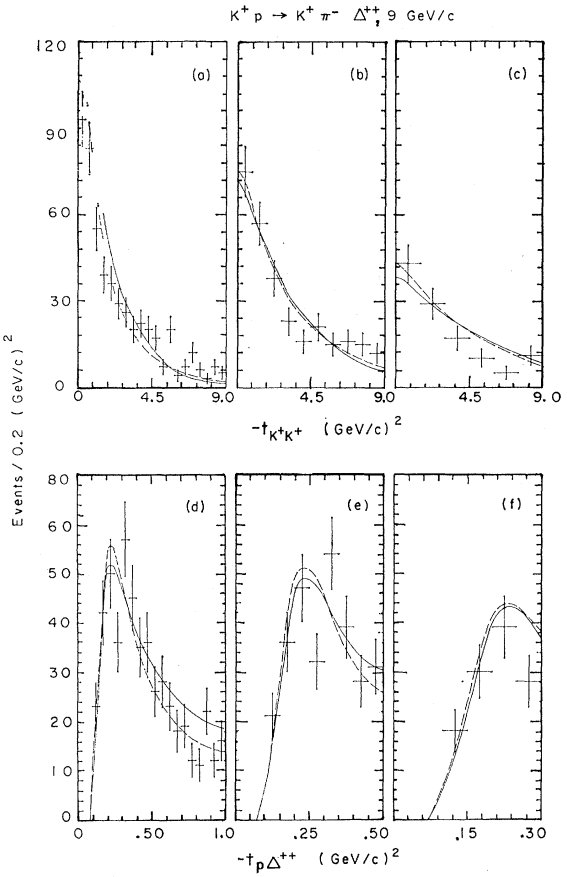

FIG. 5. $-t_{K^+K^+}$ distributions for samples (a) A, (b) B, and (c) C and $-t_{p\Delta^{++}}$ distributions for samples (d) A, (e) B, and (f) C. The curves have the same meaning as those shown in Fig. 4.

to be a general trend shown also in the other distributions we discuss later.

Figures 4(a)–4(c) and Figs. 4(d)–4(f) show the $\Delta^{++}\pi^-$ mass distributions and the $K^+\Delta^{++}$ mass distributions. In Fig. 4(a) the data peak at around 1500 MeV, where there are three $I=\frac{1}{2}$ baryonic resonances, P_{11}, D_{13}, and S_{11}.[8] The calculated curves peak at about 80 MeV above 1500 MeV. However, in Figs. 4(b) and 4(c) the curves agree with the data. The curves from the model shift their peak by 80 MeV in the $\Delta^{++}\pi$ mass from Fig. 4(a) to Figs. 4(b) and 4(c), yet the data do not show such an apparent change. This indicates that the model may very well apply to small-t regions (e.g., samples B and C) but does not apply to the large-t regions (e.g., sample A). Similar disagreements also show in some of the distributions from sample A discussed in the following paragraphs. In Fig. 4(d) the dashed curve agrees with the data better than the solid curve, but it is not so obvious in Figs. 4(e) and 4(f).

Figures 5 and 6 show the distributions of $-t_{KK}$ and $-t_{p\Delta}$, and $-t_{K\pi}$ and $-t_{p\pi}$. Except for $-t_{p\pi}$ in Figs. 6(e) and 6(f), in general the model (for both case I and case II) agrees well with the data.

Figure 7 shows the decay angular distributions for the $K^+\pi^-$ system in its rest frame. The $\cos\theta$ distributions [Figs. 7(a)–7(c)] are plotted from 0 to 1.0 since there are no events from the data and the model in the backward region. As the t cuts decrease, the events are populated in an even smaller forward region [e.g., $\cos\theta(K^+\pi^-)\gtrsim 0.7$ for both $-t_{KK}$ and $-t_{p\Delta}$ less than 0.3 $(\mathrm{GeV}/c)^2$]. The Treiman-Yang angular distribution [Figs. 7(d)–7(f)] becomes flatter as $t_{p\Delta}$ decreases. This indicates that the Treiman-Yang angular distribution tends to agree with the well-known prediction of single-pion particle exchange in the limit of very small $-t_{p\Delta}$.[9] The solid curve and the dashed curve show considerable discrepancy between them in Fig. 7(d) (sample A). Otherwise, for both case I and case II the model agrees with the data rather well.

Figure 8 shows the distributions of $\cos\theta$ and ϕ for the $\Delta^{++}\pi^-$ system. Again a large discrepancy between the curves is observed in large-t regions [Figs. 8(a) and 8(d)]. Figure 9 shows the Toller-angle distributions.

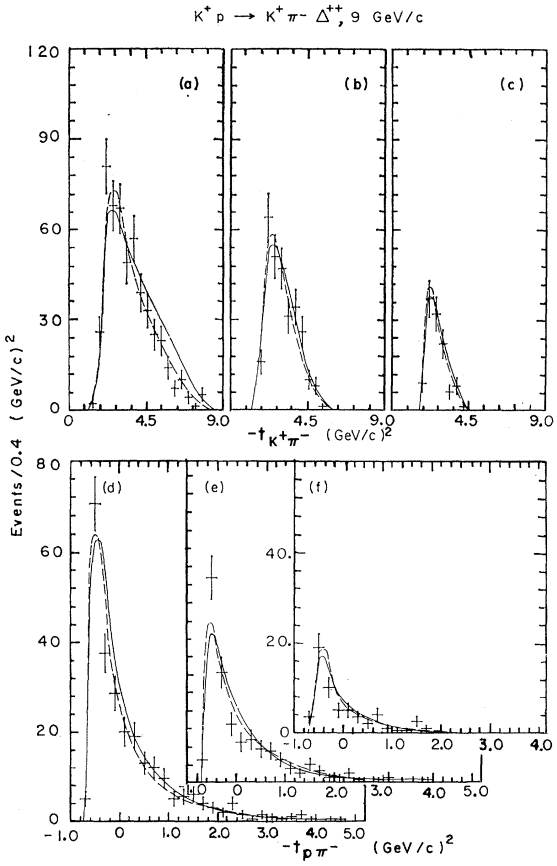

FIG. 6. $-t_{K^+\pi^-}$ distributions for samples (d) A, (e) B, and (f) C. The curves have the same meaning as those shown in Fig. 4.

[8] Particle Data Group, Rev. Mod. Phys. 42, 87 (1970).

[9] S. B. Treiman and C. N. Yang, Phys. Rev. Letters 8, 140 (1962).

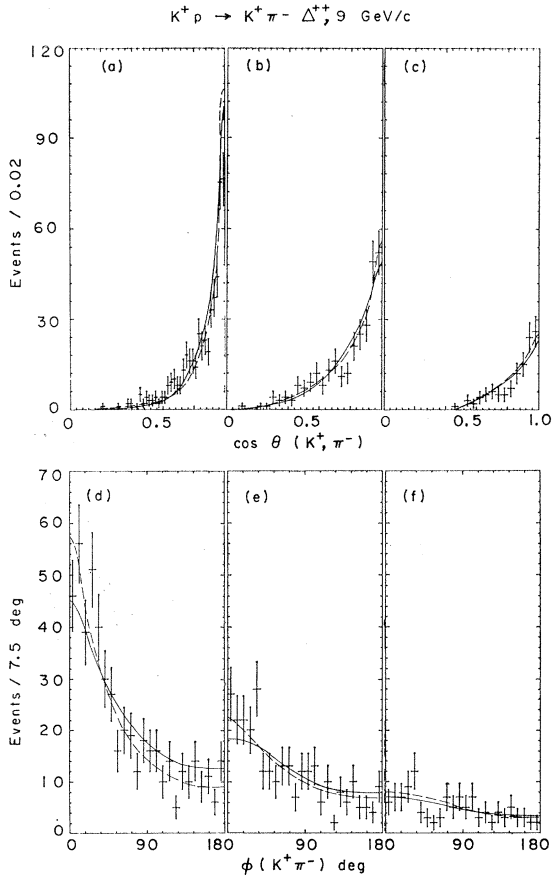

FIG. 7. $\cos\theta(K^+\pi^-)$ distributions for samples (a) A, (b) B, and (c) C and $\phi(K^+\pi^-)$ distributions for samples (d) A, (e) B, and (c) C. $\theta(K^+\pi^-)$ are the Jackson angle and the Treiman-Yang angle for the $K^+\pi^-$ system. The curves have the same meaning as those shown in Fig. 4.

The model agrees with the data fairly well for sample B, but does not agree with the data in both the large-t region (sample A) and *the small-t region (sample C)*. The dash-dot lines in Fig. 9 represent the phase space which is *normalized to each sample*. It strongly peaks near $\omega=180°$. At $\omega=180°$, the two particles in the initial state and the three particles in the final state lie in the same plane. As the t cuts decrease, the phase-space curve gets closer to the results of the model and the data points.

The χ^2 values of the various distributions for sample B are given in Table I. Table I indicates the following.

(1) Over all the kinematical variables studied, the confidence level of case II is more uniform than that of case I. Consider the latter. If one happens to choose to fit the distributions of $M(K^+\pi^-)$, $M(K^+\Delta^{++})$, $-t_{p\Delta}$, and $-t_{K\pi}$, one may claim very good agreement between the model and the data. On the other hand, if one chooses the variables $M(\Delta^{++}\pi^-)$, $-t_{KK}$, $-t_{p\pi}$, and the Toller angle ω, one may consider that the model is a failure. The results could be even worse if only some of the distributions from sample A were considered.

TABLE I. χ^2 values for sample B.[a]

Distribution	χ^2	d.f.[b]	Confidence level (%)	χ^2	d.f.[b]	Confidence level (%)
$M(K^+\pi^-)$	8.1	14	88.3	16.1	13	17.1
$M(\Delta^{++}\pi^-)$	18.3	11	7.3	15.2	10	12.5
$M(K^+\Delta^{++})$	8.7	9	46.4	10.8	8	21.5
$-t_{KK}$	20.8	6	0.2	11.4	5	4.4
$-t_{p\Delta}$	3.8	3	27.9	3.5	2	17.7
$-t_{K\pi}$	5.9	5	31.5	6.1	4	19.1
$-t_{p\pi}$	20.3	7	0.5	12.9	6	4.5
$\cos\theta(K^+\pi^-)$	22.2	12	3.5	12.9	11	29.4
$\phi(K^+\pi^-)$	23.3	17	14.1	19.6	16	23.9
$\cos\theta(\Delta^{++}\pi^-)$	32.3	15	0.6	19.3	14	15.3
$\phi(\Delta^{++}\pi^-)$	28.2	12	0.8	18.0	11	11.5
Toller angle ω	29.1	10	1.2	15.8	9	7.0

[a] See Ref. 6. [b] Degrees of freedom.

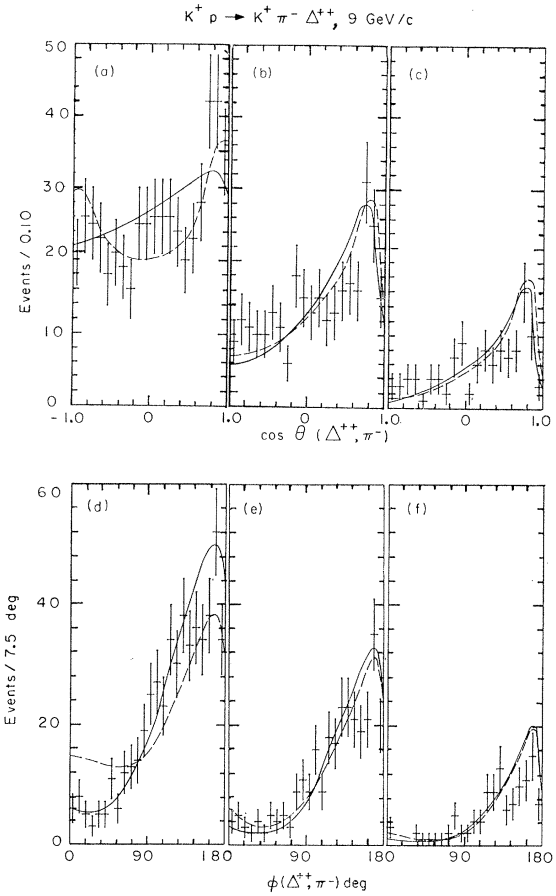

FIG. 8. $\cos\theta(\Delta^{++}\pi^-)$ distributions for samples (a) A, (b) B, and (c) C and $\phi(\Delta^{++}\pi^-)$ distributions for samples (d) A, (e) B, and (f) C. $\theta(\Delta^{++}\pi^-)$ and $\phi(\Delta^{++}\pi^-)$ are the Jackson angle and the Treiman-Yang angle for the $\Delta^{++}\pi^-$ system. The curves have the same meaning as those shown in Fig. 4.

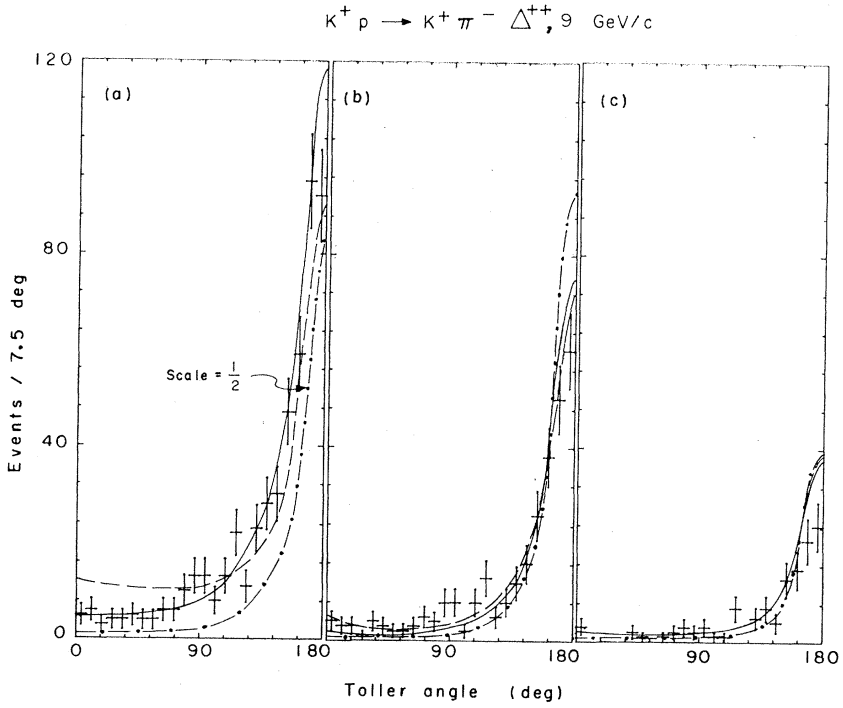

FIG. 9. Toller-angle distributions for samples (a) A, (b) B, and (c) C. The solid and the long-dash curves have the same meaning as those shown in Fig. 4. The dash-dot curve indicates the space normalized to each sample.

(2) The agreement between the model and the data is poor for the distributions of $-t_{KK}$, $-t_{p\pi}$, and ω.

B. Quantitative Analysis

A comparison of the number of events from the model and the phase space with the data under different kinematical criteria is shown in Table II. The normalization was described in Sec. II B.

We observe the following.

(1) Comparing the numbers from the data and those from the phase space, one can easily see the peripheral nature of the data.

(2) For $M(K^+\pi^-) \gtrsim 1540$ MeV, the number of events from the data agrees with the result of the model for both case I and case II. The model completely disagrees with the data in the low-$K^+\pi^-$-mass region [$M(K^+\pi^-) < 1540$ MeV] as we expect (because of the strong K^* resonance production). One important point to note is that the predictions of case I and case II disagree in this $K^+\pi^-$ mass region also.

IV. EXTRAPOLATION OF MODEL TO SMALL SUBENERGIES

In this section we discuss (a) the importance of the contribution from the extrapolation, (b) the reliability of the extrapolation with the present knowledge of Regge parameters, and (c) the isospin structure of the $K\pi$ system on the basis of (P,π) exchange in the model.

(a) In order to demonstrate the contribution from the double-peripheral process by extrapolation, in Figs. 10(a), 10(b), and 10(c) we plot the complete $K^+\pi^-$ mass spectra under the t cuts, $-t_{KK}$ and $-t_{p\Delta}$ less than 1.0, 0.5, and 0.3 $(\mathrm{GeV}/c)^2$, respectively. The curves shown in Figs. 10(a)–10(c) are the same as those shown in Figs. 3(a)–3(c). The extrapolation of the model to the small $K\pi$ mass region as shown by the dashed curves in Fig. 10 does not describe the data in the K^*_{890} resonance region, even in a crude average sense. This seems to favor the Harari postulate[10] that Pomeranchukon exchange is responsible for the background only. The double-peripheral process would contribute at least

TABLE II. Comparison of the number of events from the model and the phase space with the data under different kinematical criteria.

	$M(K^+\pi^-) \gtrsim 1540$ MeV			$M(K^+\pi^-) < 1540$ MeV		
	Sample A	Sample B	Sample C	$-t_{KK}$ and $-t_{p\Delta}$ <1.0 $(\mathrm{GeV}/c)^2$	$-t_{KK}$ and $-t_{p\Delta}$ <0.5 $(\mathrm{GeV}/c)^2$	$-t_{KK}$ and $-t_{p\Delta}$ <0.3 $(\mathrm{GeV}/c)^2$
Data	511	287	115	1804	1375	953
Case I	536	287	127	327	307	251
Case II	500	287	132	461	404	318
Phase space	1805	287	54	2565	824	330

[10] H. Harari, Phys. Rev. Letters **20**, 1395 (1968).

30–60% of the background in the low $K\pi$ mass region [$M(K^+\pi^-)<1540$ MeV]. Owing to the $e^{\gamma t_{KK}}$ factor in Eq. (3a), the model yields a large intensity in the forward $\theta(K^+\pi^-)$ region even in the low $K\pi$ mass region (except near the $K\pi$ threshold). This contributes to part of the well-known forward-backward asymmetry in the $K\pi$ system.[11] Ignoring the isospin structures, calculations involving a p-wave K^*_{890} and a d-wave K^*_{1420} with a coherent and an incoherent double-peripheral process with (P,π) exchange have been tried. They do not reproduce some of the important features in $K\pi$ asymmetry as a function of $K\pi$ mass. Since the contribution from the extrapolation to the background is large and yet it cannot account for all the background beside the two well-established K^*'s, one may ask whether the double-peripheral process or the K^* resonance productions can be isolated from the data in order to obtain a relatively clean sample. The answer to this question is no, because *both processes are dominated by pion exchange and favor small* $-t_{p\Delta}$.

(b) In Table II the numbers of events in the low $K\pi$ mass region from the extrapolation of the model differ by about 30% between case I and case II. This is a typical fluctuation, introduced to a certain extent by the uncertainties of the parameters used in Eq. (3a). With the present knowledge about Regge parameters and the statistical level of the data, one cannot determine how much each exchange pair (discussed in Sec. II A) contributes, or whether one should try to find a better new model. Hence, at the present stage, the extrapolation of the model can only offer a qualitative description for the data.

(c) Based on an isospin argument in Ref. 1, it was concluded that the low $\Delta^{++}\pi^-$ mass enhancement is predominantly of $I=\frac{1}{2}$. This isospin assignment favors an $I=0$ object exchanged at the $K^+_{\text{in}}K^+_{\text{out}}$ vertex. Among all the allowed exchange pairs (see Sec. II A) the P is the only candidate with $I=0$.

In fact we obtain $C\approx 0.85$, which is close to unity, in this analysis. This agrees with the assumption that P is the dominant object exchanged at the K^+K^+ vertex. Comparing (P,π) and (P,A_1), if one assumes that α_π and α_{A_1} have the same slope, then A_1 would be a lower trajectory and its pole would be farther away from the physical region than the pion pole. Hence the contribution of A_1 is less important than that of π. If one assumes π and A_1 degeneracy, then there should be no essential difference regardless of whether (P,A_1) is included in addition to (P,π). The comparison of the model and the data also indicates that our (P,π) assumption is rather good, at least in the region where $-t_{KK}$ and $-t_{p\Delta}$ are small. These arguments justify the assumption that the (P,π) exchange pair dominates the double-peripheral process. Then one can further study the upper part of the diagram in Fig. 1(b) as a K^+_{in} scattered by a virtual pion producing the $K^+\pi^-$ final state with P exchanged in the t channel. By isospin crossing,[12] for the reaction $K^+\pi^-\to K^+\pi^-$ via an $I=0$ object exchanged in the t channel, the $I=\frac{3}{2}$ and $I=\frac{1}{2}$

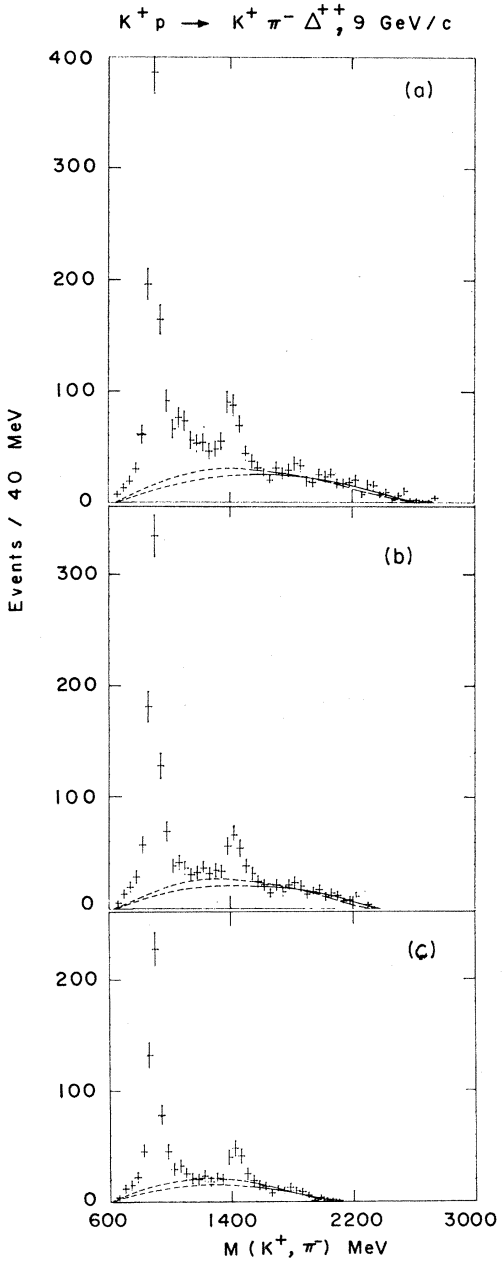

FIG. 10. $K^+\pi^-$ mass distributions with $-t_{K^+K^+}$ and $-t_{p\Delta^{++}}$ less than (a) 1.0 (GeV/c)^2, (b) 0.5 (GeV/c)^2, and (c) 0.3 (GeV/c)^2. The solid and the dashed curves have the same meaning as those shown in Fig. 3.

[11] (a) An earlier discussion has been given by C. Fu, A. Firestone, G. Goldhaber, and G. H. Trilling, Bull. Am. Phys. Soc. **14**, 560 (1969); see also Ref. 1; (b) C. Fu, A. Firestone, G. Goldhaber, G. H. Trilling, and B. C. Shen, LRL Report No. UCRL-18201, 1968 (unpublished).

[12] Huan Lee, J. Math. Phys. **10**, 779 (1969).

parts of the amplitude are in the ratio 1:2. The implications of this are that we cannot neglect the $I=\frac{3}{2}$ component in doing the analysis for the $K\pi$ system in the low $K\pi$ mass region. Whether the $K\pi$ asymmetry can be explained by including the $I=\frac{3}{2}$ component is completely unclear.

V. CONCLUSIONS

(1) (P,π) exchange dominates the reaction $K^+p \to K^+\pi^-\Delta^{++}{}_{1236}$ at 9 GeV/c for $M(K^+\pi^-) \gtrsim 1540$ MeV. In general the model agrees with the data fairly well for $-t_{KK}<0.5(\mathrm{GeV}/c)^2$ and $-t_{p\Delta}$ $0.5(\mathrm{GeV}/c)^2$. The validity of the model above these t cuts is definitely in doubt.

(2) The introduction of an empirical Toller-angle dependence at the interval vertex helps to improve the confidence level to be more uniform over the distribution of all the variables considered except that the fit to the Toller-angle distribution itself has not been improved much. In the small-t region, the Toller-angle distribution [as shown in Fig. 9(c)] indicates a large discrepancy between the model and the data. Further investigation of Toller-angle dependence is necessary.

(3) With the present knowledge of the Regge parameters determined by the data from the two-body final states, the many possibilities of the exchange pairs, and the statistical limitation of our data, the values of the Regge parameters we used are subject to quite large uncertainties. However, this should not affect the conclusion that the contribution from the extrapolation is large. By comparing tke data with the result from the extrapolation to the small $K\pi$ mass region, we find that the latter agrees with Harari's postulate that Pomeranchukon exchange is responsible for the background only.

ACKNOWLEDGMENTS

I thank Professor G. Goldhaber, Dr. E. L. Berger, Dr. A. Firestone, and Dr. P. D. Ting for their critical comments and discussions. I thank Professor G. H. Trilling for reading the manuscript. I thank Dr. R. Shutt and the staff of the 80-in. bubble chamber and Dr. H. Foelsche and the AGS staff at Brookhaven for helping with the exposure. I am also thankful for the valuable support given by the White and the FSD staff and by our programming and scanning staff, in particular, Emment R. Burns.

PHYSICAL REVIEW D VOLUME 3, NUMBER 1 1 JANUARY 1971

Regge-Pole-Cut Analysis of Total Cross Sections with $SU(3)$ and Exchange Degeneracy*

JANE C. JACKSON
Department of Physics, Arizona State University, Tempe, Arizona 85281
(Received 27 April 1970)

A phenomenological study of $SU(3)$ and exchange degeneracy is made in a Regge-pole-cut model. The high-energy data of pion-nucleon, kaon-nucleon, nucleon-nucleon, and nucleon-antinucleon total cross sections, including the new Serpukhov data, are analyzed by means of least-squares fits with parameters corresponding to the P, P', ρ, A_2, and ω Regge poles and subtractive vacuum cut. The data are fitted adequately with the assumptions of $SU(3)$ and exchange degeneracy. For completeness, the data are analyzed with the assumptions of $SU(3)$ alone, exchange degeneracy alone, and also without either of these assumptions.

I. INTRODUCTION

PRESENTED is a Regge-phenomenological study of $SU(3)$ and exchange degeneracy, utilizing the available high-energy total-cross-section data of meson-nucleon, nucleon-nucleon, and nucleon-antinucleon reactions, using a model consisting of Regge poles and a vacuum cut. A similar study, although involving only Regge poles and with slightly different pole assumptions, was made by Ahmadzadeh[1] some four years ago, with notable success. The recent Serpukhov data[2] with its surprises makes a study similar to that of Ref. 1 [i.e., using Regge poles with $SU(3)$ and exchange degeneracy], but including a vacuum cut, of interest. Phenomenological studies of the total cross sections have already been made by Barger and Phillips[3] and by Lendyel and Ter-Martirosyan.[4] However, they did not include $SU(3)$ or exchange degeneracy in their analyses.

II. FORMALISM

Specifically, the five leading Regge poles, the P (Pomeranchukon), P', ω, ρ, and A_2, are included in the present analysis. The ϕ and f' poles are assumed to de-

* Research supported in part by the U. S. Air Force Office of Scientific Research, Office of Aerospace Research, under Grant No. AF-AFOSR-7125-977.

[1] A. Ahmadzadeh, Phys. Rev. Letters **16**, 952 (1966).

[2] IHEP-CERN Collaboration, Phys. Letters **30B**, 500 (1969).

[3] V. Barger and R. J. N. Phillips, Phys. Rev. Letters **24**, 291 (1970).

[4] A. I. Lendyel and K. A. Ter-Martirosyan, in Proceedings of the International Conference on High-Energy Physics and Theory of Elementary Particles, Kiev, 1969 (unpublished).